Unimolecular Micelle Formation of Poly(methyl methacrylate)-*graft*-polystyrene in Mixed Selective Solvents of Acetonitrile/Acetoacetic Acid Ethyl Ether

Atsushi Kikuchi and Takuhei Nose*

Department of Polymer Chemistry, Tokyo Institute of Technology, Ookayama, Meguro-ku, Tokyo 152, Japan

Received March 29, 1996; Revised Manuscript Received July 25, 1996[⊗]

ABSTRACT: Unimolecular micelle formation is investigated by means of light scattering for poly(methyl methacrylate)-*graft*-polystyrene copolymers with low grafted chain densities in dilute solution of mixed selective solvents. Molecular weights of poly(methyl methacrylate) (PMMA) backbone and polystyrene (PS) branch are about 6×10^6 and 9×10^3 g mol^{-1}, respectively, and the grafted chain density ranges from 6 to 17 wt % in terms of PS composition. The mixed solvents are marginally good solvents for PMMA and are nonsolvents for PS. From the results of static and dynamic light scattering measurements as a function of temperature and solvent composition, it is demonstrated that, at higher branch densities and lower temperatures, the rod like unimolecular micelles are formed, made of a few linearly connected flowers with small cores of associated PS branches and petals of PMMA backbone chain. The number of petals per flower increases with increasing branch density and decreasing solubility of solvents for PMMA. On the other hand, at the lowest branch density of 6 wt %, instead of unimolecular micelle formation, intermolecular associations take place, even at low copolymer concentration.

Introduction

Micellization of diblock and triblock copolymers in selective solvents have been studied extensively from both theoretical and experimental viewpoints.[1−8] On the other hand, a limited number of studies on multiblock copolymers including graft copolymers have been reported,[9−14] although a variety of micellar structures may be expected. One of the unique properties of the multiblock copolymers is their ability to form unimolecular micelles with intramolecular associations, which are not seen in low-molecular-weight surfactants.

In this series of studies, we are concerned with the structures of the unimolecular micelle of a graft copolymer molecule which consists of a long backbone and short branches with low grafted chain density. Expected structures are illustrated as a function of solvent qualities of the backbone chain and the branch chains in Figure 1.[15] In a previous paper,[15] we studied region 1 of this figure, i.e., the unimolecular micelle formation of poly(methyl methacrylate)-*graft*-polystyrene (PMMA-*g*-PS) in isoamyl acetate, which is a good solvent for branched PS and a theta (Θ) solvent for PMMA backbone, and concluded that unimolecular micelles were formed by intramolecular segregation between the PMMA backbone and PS branches, where the shrunken PMMA backbone formed a rodlike core covered with PS chains. In the present work, we focus our attention on region 2, i.e., unimolecular micelles in selective solvent having opposite solvent selectivity, that is, solvent selective for the backbone. In this region, formation of flower-like and/or flower-connecting-type unimolecular micelles are expected.

Halperin theoretically predicts that a copolymer of multiblocks connecting alternately forms a unimolecular micelle of the flower type or a flexible string of the flowers in selective solvent.[14] Semenov et al. expect a collapsed chain of flowers, forming a compact globule, for the structure of a unimolecular micelle of such a multiblock copolymer instead of a swollen chain of flowers.[16] de Gennes also predicts unimolecular micelle formation of the flower type for statistical copolymers.[17]

In this study, we use the same PMMA-*g*-PS copolymers as those in the previous study and choose mixtures of acetonitrile (AN)/acetoacetic acid ethyl ether (AAEE) as selective solvent, which are marginally good solvents for PMMA and nonsolvents for PS. Static and dynamic light scattering measurements have been carried out on their dilute solutions to investigate the formation and the structure of unimolecular micelles.

Experimental Section

Materials. In Table 1 are listed characteristics of the graft copolymers, PMMA-*g*-PS, used in this study. Details of preparation and characterization of these graft copolymers were described in previous papers.[15,18] CL-1 and CL-2, which have been synthesized by coupling reaction between fractionated PMMA (CL-b) and living PS, have the same backbone chain length and almost the same branch length with narrow molecular weight distribution, but they have different branch densities. Molecular weight distribution and chemical composition distribution of the CL series are very narrow, while those of RS-8, which have been made by using macromonomers, are not so narrow in comparison. In Table 2 are listed the values of average number, m, of branches and average molecular weight, M_{sc}, between nearest-neighbor branch points. The branch number m ranges from 40 to 140, and the molecular weight M_{sc} is 4−14 times larger than the molecular weight of the branches.

Polystyrene used in cloud point measurements was a product of Pressure Chemical Co., with nominal molar mass and polydispersity index of 8×10^2 g mol^{-1} and 1.3, respectively, and is here coded as PSc.

Light Scattering Measurements. Light scattering measurements were carried out for dilute solutions of mixed solvents of acetonitrile (AN) and acetoacetic acid ethyl ether (AAEE). Purchased AN and AAEE were dried over calcium hydride and purified by distillation. Stock solutions were prepared by dissolving the graft copolymers in AAEE, followed by adding a desired amount of AN, stirring gently at room temperature for 2 h, and keeping the solutions around 60 °C for 1 day. The stock solutions were filtered through a Millipore filter into optical cells and diluted with dust-free mixed solvent to the desired concentration. Subsequently, the optical cells were flame-sealed under mild vacuum and left around 60 °C

[⊗] Abstract published in *Advance ACS Abstracts,* September 15, 1996.

S0024-9297(96)00480-9 CCC: $12.00

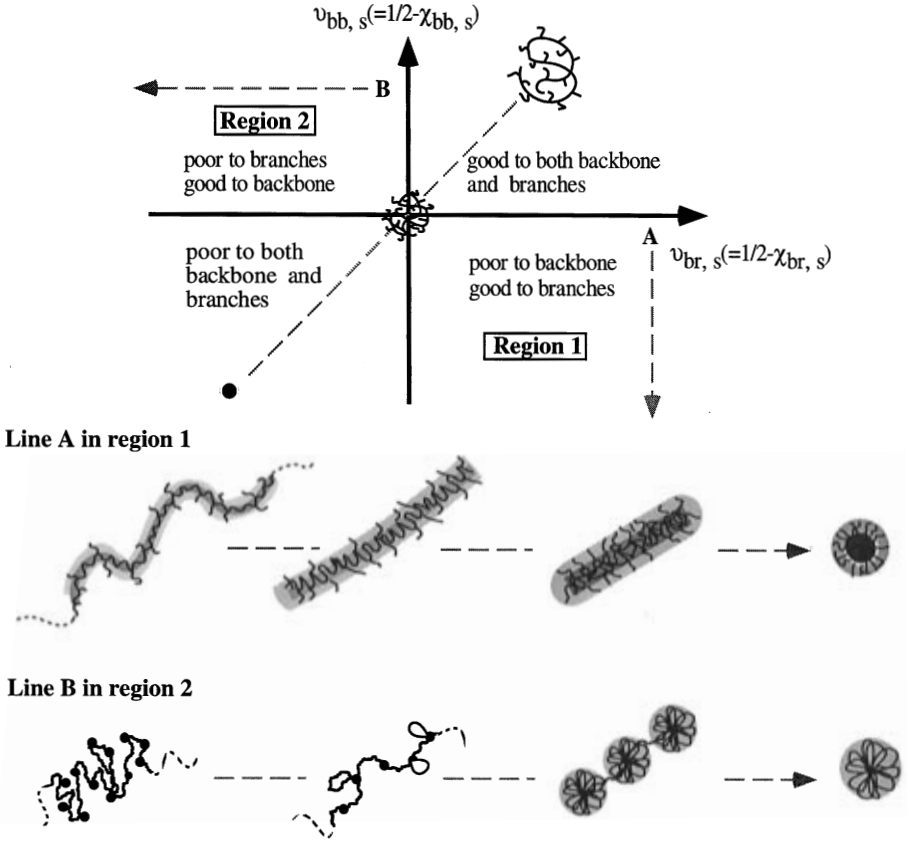

Figure 1. Schematic presentation of possible micellar structures of the graft copolymer with short branches of a low branch density as a function of solvent qualities for the backbone chain and the branch chains, which are represented by excluded volume parameters $\nu_{bb,s} = {}^1/_2 - \chi_{bb,s}$ and $\nu_{br,s} = {}^1/_2 - \chi_{br,s}$, respectively, where χ is the monomer−monomer interaction parameter. Change of nonselective solvent quality is presented by the line $\nu_{bb,s} = \nu_{br,s}$, where the coil−globule transition observed in ordinary linear polymers will occur. If solvent quality for the backbone polymer changes from nearly Θ condition ($\nu_{bb,s} \cong 0$) to nonsolvent quality ($\nu_{bb,s} \ll 0$), keeping solvent quality for the branch chains good (line A in region 1), a unimolecular micelle of wormlike chain will appear, followed by cylindrical and spherical unimolecular micelles, where the backbone is covered with branch chains. In region 2, as the solvent quality for the branches becomes poorer from nearly Θ condition ($\nu_{br,s} \cong 0$) at a fixed $\nu_{bb,s}(>0)$ solvent (line B in region 2), a unimolecular micelle of flower-connecting type will be formed via random coil structure with shrunken branch chains and/or loops. In the nonsolvent quality limit ($\nu_{br,s} \ll 0$), a unimolecular micelle made up of one flower will be formed.

Table 1. Characteristics of PMMA-*g*-PS Samples

	backbone (CL-*b*)		branch		average PS composition,[c] ⟨W⟩
sample	M_w,[a] 10^6 g mol^{-1}	M_w/M_n[b]	M_w,[b] 10^3 g mol^{-1}	M_w/M_n[b]	
CL-1	5.58	<1.10	8.77	1.07	0.0614
CL-2	5.58	<1.10	9.19	1.04	0.128
RS-8	5.96		8.52	1.10	0.175

[a] Measured by static light scattering. [b] Measured by SEC. [c] Measured by ^{1}H NMR.

Table 2. Average Number, *m*, of Branches per Molecule and Average Molecular Weight, M_{sc}, between Nearest-Neighbor Branch Points

sample	*m*[a]	M_{sc},[b] 10^4 g mol^{-1}
CL-1	42.6	13.4
CL-2	93.2	6.26
RS-8	137	4.03

[a] Calculated from $M_w\langle W\rangle/M_w$(branch). M_w of CL-1, CL-2, and RS-8 are 6.09×10^6, 6.69×10^6, and 7.22×10^6 g mol^{-1}, respectively, where ⟨W⟩ is the average PS composition. [b] Calculated from $M_w(1 - \langle W\rangle)/m$.

for 1 day to stabilize the solution before light scattering measurements.

The light scattering apparatus was specially designed, with an Ar ion laser operating at a wavelength of 488 nm as light source, using the photon counting method. A correlator used in dynamic light scattering was a Multiple Tau Digital Correlator, ALV-5000. Details of the light scattering spectrometer have been described elsewhere.[19]

The excess Rayleigh ratio ($R_{vv}(\theta)$) for vertically polarized incident and scattered light as a function of concentration (C) and angle (θ) was analyzed by Zimm plots to determine the molecular weight, M_w, the radius of gyration, R_g, and the second virial coefficient, A_2, on the basis of the equation

$$\frac{KC}{R_{vv}(q)} = \frac{1}{M_w}\left[1 + \frac{R_g^2}{3}q^2 + \cdots\right] + 2A_2C + \cdots \qquad (1)$$

where the constant K is given by $K = 4\pi^2n^2(\partial n/\partial C)^2/(N_A\lambda_0^4)$, with n being the refractive index of solvent, N_A the Avogadro constant, $(\partial n/\partial C)$ the refractive index increment, and λ_0 the wavelength of the incident beam in vacuum, and the momentum transfer q is given by $q = (4\pi n/\lambda_0)\sin(\theta/2)$. The concentration C is in weight per volume of solution.

The above conventional analysis could not be used in most of the present systems because intermolecular associations occur at relatively high concentrations. In these cases, we evaluated apparent values of M_w and R_g without the extrapolation, which were defined as

$$M_w = R_{vv}(0)/KC \qquad (2)$$

$$R_g^2 = \frac{M_w(\text{initial slope})}{q^2/3} \qquad (3)$$

where $KC/R_{vv}(0)$ and (initial slope) are the intercept and the initial slope of $KC/R_{vv}(\theta)$ vs q^2 plots at a finite concentration. Since the polymer concentration was low ($<2 \times 10^{-4}$ g (g of

solution)$^{-1}$) enough, the apparent values thus obtained were treated as true ones.

The value of R_g is the refractive-index-increment-weighted one in copolymers.[20] In the present case, however, the scattered light intensity of the PMMA backbone dominates over that of the PS branches because of the low branch composition, so the obtained R_g can practically be regarded as a true radius of gyration of the *z*-average.

For a copolymer solution with polydispersity in chemical composition, the values of M_w and R_g obtained by the conventional way are apparent, depending on the refractive indexes of the solvents. Although this is the case for the copolymer RS-8, the apparent value of R_g is used without any correction because the polydispersity is not so large.[18] The apparent values may more strongly reflect the components of larger PS compositions having the larger refractive index increment.

Refractive indexes and densities of the solvents were obtained from reported values with corrections for wavelength and temperature.[21,22] The refractive index increments were measured with a differential refractometer (Union Giken RM-102) for PMMA and the graft copolymers.

The correlation function of electric field obtained from the autocorrelation function of scattered light intensity approximately followed a single-exponential decay and allowed us to obtain the decay rate, Γ, by the second-order cumulant method.[23] The Γ value showed q^2 dependence because all the experimental conditions satisfied that $R_g q < 1$, so the diffusion coefficient D was evaluated by $D = \Gamma/q^2$. The obtained D was transformed to the hydrodynamic radius, R_h, by the Einstein–Stokes equation,

$$R_h = kT/6\pi\eta D \tag{4}$$

where k, T, and η are the Boltzman constant, absolute temperature, and solvent viscosity, respectively. The viscosity η was measured with an Ubbelohde-type viscometer as a function of temperature and solvent composition. Although D values should be those at the infinitely dilute limit, diffusion coefficients D at a very low but a finite concentration ($< 2 \times 10^{-4}$ g (g of solution)$^{-1}$) were used here, and the apparent values thus obtained were regarded as true ones.

Experimental Results

Solvent Quality of Mixed Solvents to PMMA and PS. Compositions of the mixed solvents were [AN]:[AAEE] = 2:1 and [AN]:[AAEE] = 3:1, where [X] is the concentration of X in weight. These solvent compositions are abbreviated by 21 or 31, adding to the sample code as CL-b-21 and CL-b-31, for example, for denoting the system. Figure 2 shows R_g and A_2 of CL-b in the mixed solvents, along with those of CL-b in a thermodynamically good solvent and at the Θ condition.[15] The results indicate that these solvents are marginally good for the backbone PMMA. The higher AAEE content solvent shows better solvent quality for PMMA. It is found that the Θ temperature for the CL-b-31 system is located a little below 10 °C, while the Θ temperature for pure AN is around 40 °C.[24]

Figure 3 represents cloud points for PSc-21 and PSc-31 systems as a function of polymer concentration. Even the low-molecular-weight PSc cannot be dissolved in these solvents at 82 °C around 35 wt % PSc. The Flory–Huggins interaction parameter, χ_c, of the PSc solution at the critical point is evaluated by the equation

$$\chi_c = {}^1/_2\left(1 + \frac{1}{\sqrt{N}}\right)^2 \tag{5}$$

to be 0.926 per PS monomer, so that the χ parameter for both solutions should be larger than 0.926. Here, N is the polymerization index. Therefore, noting that $\chi = {}^1/_2$ at the Θ temperature, these mixed solvents are obviously *non*solvent for PS branches.

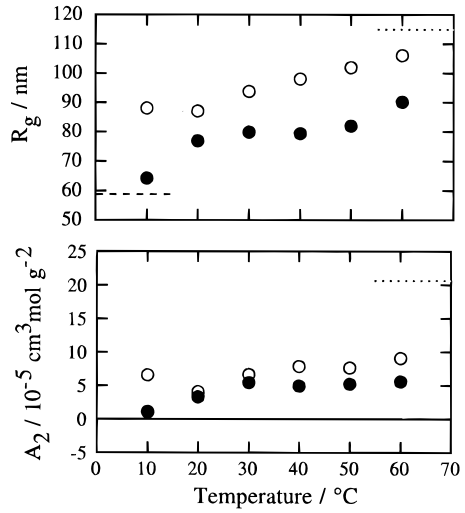

Figure 2. Temperature dependence of R_g and A_2 of CL-b in AN/AAEE mixed solvents. (○) CL-*b*-21; (●) CL-*b*-31. Dotted line and broken line indicate those values of CL-b in nonselective good solvent (1-ethylnaphthalene, 30 °C) and Θ condition (isoamyl acetate, 60 °C), respectively.

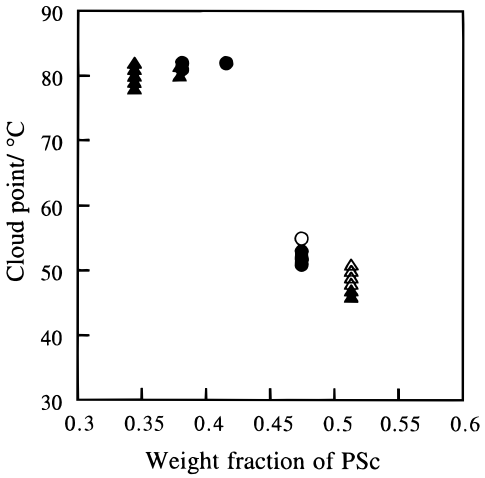

Figure 3. Cloud points for PSc-21 (○, ●) and PSc-31(△, ▲) systems as a function of polymer concentration. Open symbols, clear; filled symbols, cloudy.

R_g, R_h, and A_2 of the Graft Copolymers. Figure 4 shows the temperature dependence of M_w for the copolymers in mixed solvents, which indicates that no appreciable associations take place in any of the systems except CL-1-21. Although CL-1 has the lowest branch density (BD), its M_w increases at low temperatures (<20 °C), showing that intermolecular associations are formed even at a concentration lower than 2×10^{-4} g (g of solution)$^{-1}$. The association number is about 2 at 10 °C. Seeing the results in Figure 4 more closely, one can notice that the M_w of CL-2-31 slightly increases at lower temperatures with decreasing temperature, suggesting the presence of intermolecular associations. In fact, at concentrations higher than 5×10^{-4} g (g of solution)$^{-1}$, the intermolecular associations have clearly been observed. Details of the association behavior of CL-2-31 will be presented elsewhere.

In Figure 5 are shown the R_g values of CL-1, CL-2, RS-8, and CL-b in mixed solvents as a function of temperature. In the solvent [AN]:[AAEE] = 2:1, the copolymers CL-1, with the lowest BD, and CL-b, with

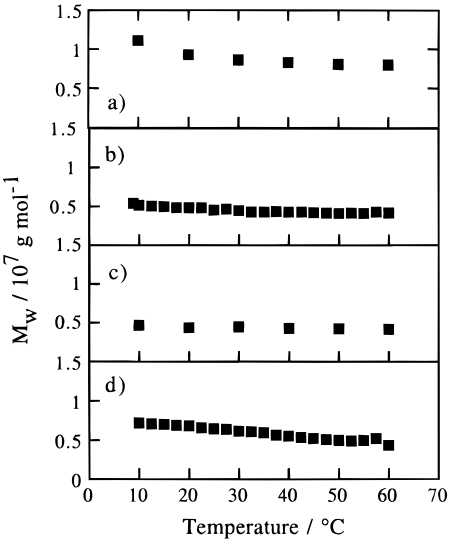

Figure 4. Change of M_w with decreasing temperature for the graft copolymers in AN/AAEE mixed solvents. (a) CL-1-21; (b) CL-2-21; (c) RS-8-21; (d) CL-2-31. Polymer concentrations are lower than 2×10^{-4} g (g of solution)$^{-1}$.

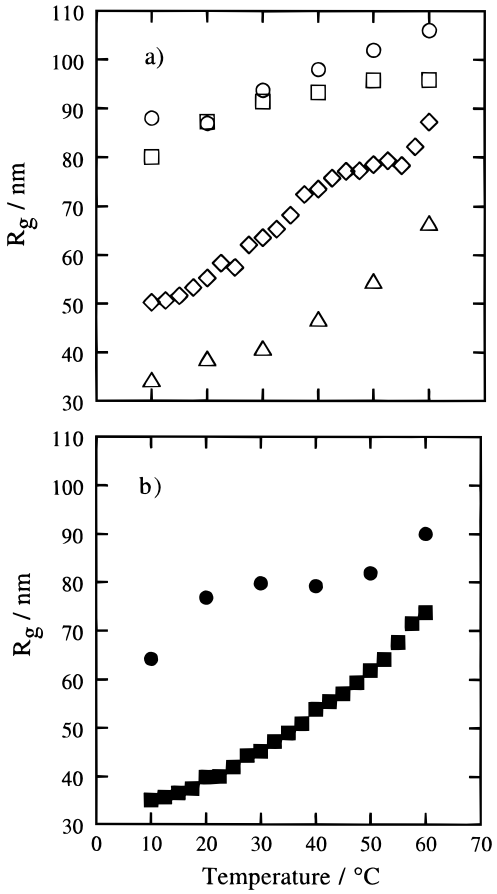

Figure 5. Temperature dependence of R_g for the graft copolymers and the backbone polymer in mixed solvents of [AN]:[AAEE] = 2:1 (a) and 3:1 (b). (○) CL-b-21; (□) CL-1-21; (◇) CL-2-21; (△) RS-8-21; (●) CL-b-31; (■) CL-2-31. Polymer concentrations of graft copolymer solutions are lower than 2×10^{-4} g (g of solution)$^{-1}$.

no branches, have similar R_g values. CL-2-21, of 12 wt % PS branches, has almost the same R_g as that of CL-b-21 at high temperatures but exhibits a rapid decrease in R_g with decreasing temperature, and the highest BD copolymer, RS-8-21, has a much smaller chain dimension, especially at lower temperatures. Similar behavior

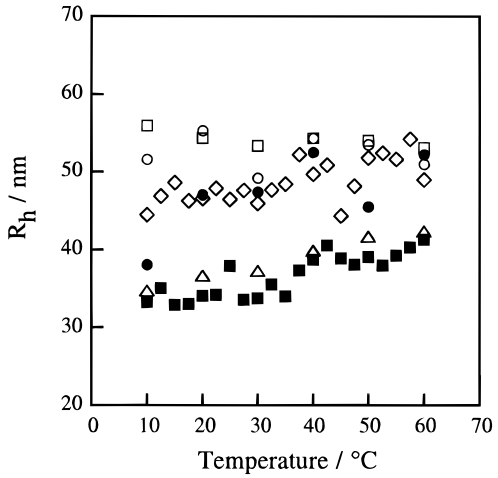

Figure 6. Temperature dependence of R_h for the graft copolymers and the backbone polymer in AN/AAEE mixed solvents. (○) CL-b-21; (□) CL-1-21; (◇) CL-2-21; (△) RS-8-21; (●) CL-b-31; (■) CL-2-31. Polymer concentrations of graft copolymer solutions are lower than 2×10^{-4} g (g of solution)$^{-1}$.

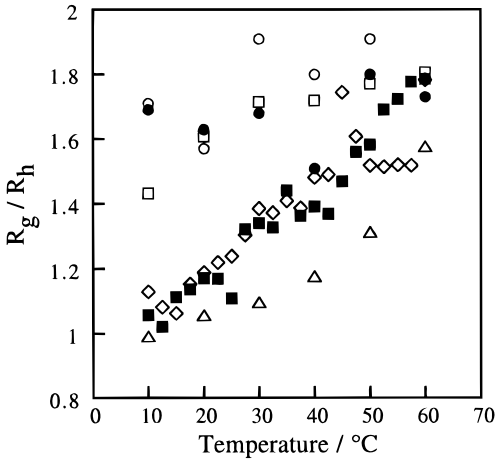

Figure 7. Temperature dependence of R_g/R_h for the graft copolymers and the backbone polymer in AN/AAEE mixed solvents. (○) CL-b-21; (□) CL-1-21; (◇) CL-2-21; (△) RS-8-21; (●) CL-b-31; (■) CL-2-31. Polymer concentrations of graft copolymer solutions are lower than 2×10^{-4} g (g of solution)$^{-1}$.

of R_g can be seen in the mixed solvent of [AN]:[AAEE] = 3:1. R_g of CL-2-31 is comparable to that of RS-8-21.

Figures 6 and 7 show the results of R_h and R_g/R_h, respectively. The ratio R_g/R_h for the lowest BD, CL-1-21, as well as those of CL-b-21 and CL-b-31, with no PS branches, ranges from 1.6 to 1.8 in the whole temperature range, showing that the chain expansion is similar to those of homopolymers. The ratios of R_g/R_h for copolymers with higher BD, CL-2-21, RS-8-21, and CL-2-31, are similar to those of CL-b at high temperatures and largely decrease with decreasing temperature, since the polymer chain shrinks and becomes compact with introduction of PS branches which are insoluble in the selective solvents. These observations are consistent with the behavior of R_g mentioned above. In Table 3 are listed numerical values of R_g, R_h, and R_g/R_h for CL-2-21, RS-8-21, and CL-2-31 at the lowest temperature, 10 °C.

For 12 wt % PS branches, CL-2, R_g and R_h decrease with increasing AN composition (see Figures 5 and 6). These changes are similar to those with decreasing temperature. However, the effects of solvent composition on the solvent quality for PMMA and PS are not equivalent to those of temperature. For example,

Table 3. R_g, R_h, and R_g/R_h of the Graft Copolymers in Mixed Solvents at 10 °C

system	R_g, nm	R_h, nm	R_g/R_h
CL-2-21	50.2	44.4	1.13
RS-8-21	34.4	34.7	0.99
CL-2-31	35.1	33.3	1.05

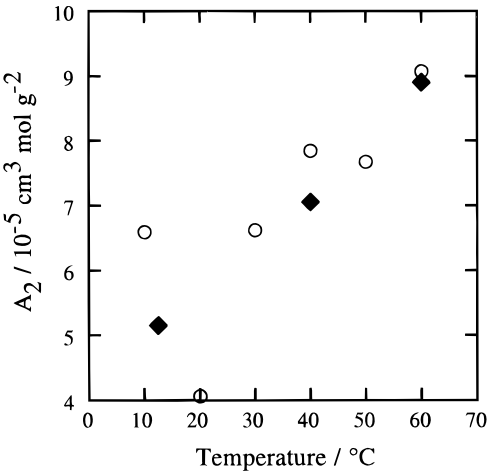

Figure 8. Temperature dependence of A_2 for CL-b-21 (○) and CL-2-21 (◆).

disagreement in R_g can be seen between CL-2-21 at 10 °C and CL-2-31 at 60 °C, where the A_2 values of PMMA backbone in both mixed solvents are almost the same (see Figure 2).

From the above findings, we can deduce the following. At the low branch composition of 6 wt %, the copolymer does not form intramolecular associates, but it takes a random coil structure with shrunken branch chains, which leads to formation of intermolecular associates at lower temperatures. In the higher BD copolymers (CL-2, RS-8), on the other hand, the formation of a unimolecular micelle with intramolecular associations is suggested by the rapid shrinkage of a whole chain with no change of M_w with decreasing temperature. The unimolecular micelle must have the small core of associated PS branches covered with the PMMA backbone chain. Formation of such a compact structure has to reflect on the second virial coefficient, that is, the interaction between two chains in solution. In Figure 8, A_2 values for CL-2-21 and CL-b-21 are plotted against temperature. These solutions have the same magnitude of A_2 in the whole temperature range, whereas R_g of CL-2 is much smaller than that of CL-b. This implies that CL-2-21 takes a more compact and repulsive particle structure, which can be represented by the penetrating function as shown in Figure 9. Here, the penetrating function ψ is defined by the equation

$$A_2 = \frac{N_A R_g^3}{M_w^2}\psi \qquad (6)$$

The function ψ of CL-b-21 has the same magnitude as that of CL-b in good solvent and a weak positive temperature dependence, whereas ψ of CL-2-21 is much larger than that of CL-b-21 and largely increases with decreasing temperature. This strongly supports the unimolecular micelle formation at lower temperatures.

Reversibility of Micellization under Cooling and Heating. Figure 10 represents the reversibility in

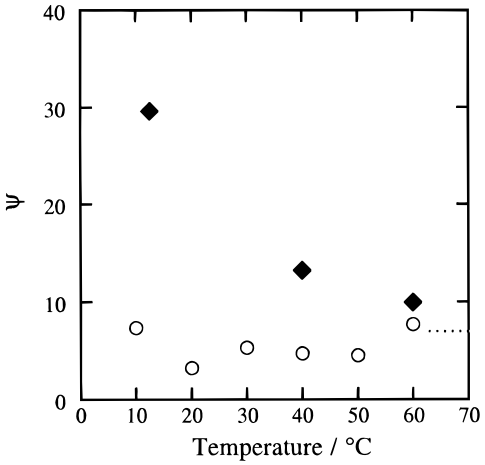

Figure 9. Temperature dependence of the penetrating function ψ for CL-b-21 (○) and CL-2-21 (◆). Dotted line indicates the ψ value of CL-b in good solvent (1-ethylnaphthalene, 30 °C).

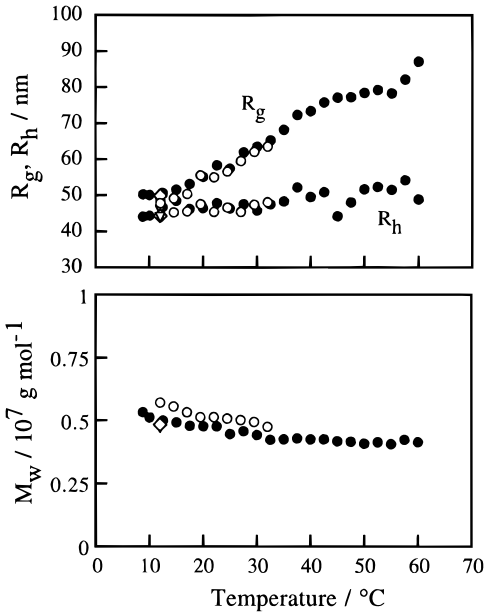

Figure 10. Change of R_g, R_h, and M_w with increasing and decreasing temperature. (●) Cooling; (○) heating; (◇) 30 min after quenching; (▼) 1.5 h after quenching. The polymer concentration is 1.43×10^{-4} g (g of solution)$^{-1}$.

changes of M_w, R_g, and R_h of CL-2-21 with cooling and heating at the rate of 2.5 °C/h. All M_w, R_g, and R_h are independent of the processes of cooling and heating, which suggests that what we have observed are quasi-equilibrium or equilibrium structures. This seems to be reasonable, because an isolated chain does not need a long time to reach the equilibrium structure.[25−28]

In the next section, we will discuss possible structures of the unimolecular micelle to determine the most likely one, and we will estimate quantitative details of the structures as a function of temperature, solvent composition, and BD.

Discussion

Comparisons with Model Structures. One of expected unimolecular micelle structures for the present system is a flower micelle, as shown in Figure 11a, which is predicted by Halperin[14] for an alternate multiblock copolymer and by de Gennes[17] for a statistical copolymer. In the present graft copolymers, the molec-

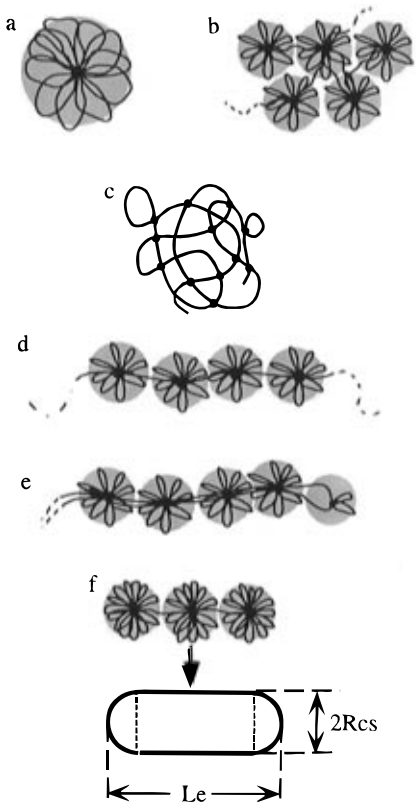

Figure 11. Schematic illustration of possible unimolecular micelle structures formed by a graft copolymer in solvent selective to the backbone chain. (a) Single flower micelle;[14,17] (b) collapsed network chain of flowers;[16] (c) four funtionally cross-linking structure; (d) flexible string of flowers;[14] (e) flexible string of flowers connected with double chains; (f) rigid string of flowers. See text for details.

ular weight, M_{br}, of PS branches is smaller than M_{sc} of PMMA subchains between the nearest-neighbor branch points (see Tables 1 and 2), so the PS branches must form a small center core in nonsolvent. Then, it is here assumed that the radius of gyration, $R_{g,flower}$, of a flower-type unimolecular micelle is similar to that of a star-shaped polymer made of arms of molecular weight $M_{sc}/2$, with the arm number f being twice the number m of petals in the flower. $R_{g,flower}$ was estimated on the basis of the fact that the ratio $g_{ga} = R_{g,star}/R_{g,arm}$ depends on the arm number f only, where $R_{g,star}$ and $R_{g,arm}$ are the radii of gyration of the star polymer and the arm polymer, respectively.[29−34] Regarding the solvent of [AN]:[AAEE] = 2:1 as a good solvent and the solvent of [AN]:[AAEE] = 3:1 as a Θ solvent for PMMA, we calculated $R_{g,flower}$ in good solvent for CL-2-21 and RS-8-21, and $R_{g,flower}$ in the Θ solvent for CL-2-31. The radius $R_{g,arm}$ of the PMMA of molecular weight $M_{sc}/2$ in good solvent was calculated from the relation $R_g^2 = 1.13 \times 10^{-18} M_w^{1.194}$ cm^2 in benzene[35] to be 5.13 nm for CL-2-21 and 3.95 nm for RS-8-21. The radius $R_{g,arm}$ at the Θ condition was calculated from the R_g of CL-b in isoamyl acetate at the Θ temperature (60 °C),[15] with the relation $R_g \propto M_w^{0.5}$, to be 4.71 nm for CL-2-31. The values of g_{ga} were evaluated with experimental equations $g_{ga} = (1.67)^{0.5} f^{0.588-0.364}$ (in good solvent) and $g_{ga} = (1.27)^{0.5} f^{0.5-0.280}$ (in Θ solvent) for $4 \le f \le 269$ by Roovers et al.[33] The estimated value of $R_{g,flower}$ was finally obtained to be 21.4 nm for CL-2-21, 17.9 nm for RS-8-21, or 16.8 nm for CL-2-31. The observed values of R_g even at 10 °C, are about 2 times larger than the calculated values in any system (see Table 3). This result excludes a single-flower structure from possible structures.

From a theoretical consideration of micelles of telechelic polymers, Semenov et al.[16] proposed a collapsed network chain of flowers, forming a compact sphere for the conformation of isolated multiblock copolymer. The structure is illustrated in Figure 11b. On the basis of this structure, the size of the micelle has been estimated. Each flower of radius L has n_p petals. The flower number, P, per micelle is related to m and n_p as $P = m/(n_p + 1)$. The maximum value, P_{max}, of flower number is $m/2$, which corresponds to $n_p = 1$, where the structure is essentially identical with four functionally cross-linking structures like a microgel as shown in Figure 11c. Assuming L to be $R_{g,star}$ of the arm number $f = 2m/P$, the radius R_{CF} of this type of spherical unimimolecular micelle with $P \gg 1$ may be evaluated as a function of P (or n_p) using the following equation:

$$R_{CF} = P^{1/3} L \tag{7}$$

The maximum possible value of R_{CF} is given by eq 7 with $P = P_{max}$ to be 32.4 nm for CL-2-21, 28.6 nm for RS-8-21, and 25.8 nm for CL-2-31. These values are still smaller than the measured values of R_g at 10 °C by 20−30% (see Table 3). The discrepancy is somewhat smaller than that for the single-flower structure examined above. However, the number of associated PS chains at a core in the structure of $P = P_{max}$ may be too small to reduce the total interfacial area between the core and solvent sufficiently, and if P is smaller than P_{max}, i.e., the association number of PS branches at a core is larger, the discrepancy becomes larger.

Another possible structure is a flexible string of flowers, as illustrated in Figure 11d, which is also predicted by Halperin[14] for alternate multiblock copolymers. A similar structure may be formed in other ways by intramolecular associations, e.g., a string of flowers connected with double or multiple chains, as shown in Figure 11e. However, the double- or multiple-chain connection is unlikely, since it results in loss of conformational entropy, so that the single-chain connection may occur predominantly. If P is large enough, the string of flowers can be regarded as a random coil following self-avoiding or Gaussian statistics, depending on solvent quality. Then, we may estimate the radius, R_{SF}, of a flexible string of flowers as a function of P (or n_p) by

$$R_{SF} = \frac{1}{\sqrt{6}} P^{\nu} [2L] \tag{8}$$

with $\nu = 0.588$ for CL-2-21 and RS-8-21, and $\nu = 0.5$ for CL-2-31. The flower number P, which reproduces the measured value of R_g at 10 °C, is 18 for CL-2-21, 12 for RS-8-21, or 28 for CL-2-31. These values may be too small to exhibit sufficient chain flexibility, and so the micelle formed may not be a flexible string. The smaller values of ratio R_g/R_h (see Table 3) compared with those of flexible linear homopolymer CL-b also suggest more compact structures.

If P is smaller, the flexibility of this type of unimolecular micelle may almost vanish, and the shape as a whole is regarded as a rigid rod, as shown in Figure 11f. The radius, $R_{g,RR}$, of gyration of a uniform rigid rod with hemispheres at its ends is given as a function

Table 4. Contour Length, L_e, Radius of Cross Section, R_{cs}, Axis Ratio, $L_e/2R_{cs}$, and Number of Petals, n_p, per Flower for the Unimolecular Micelles[a]

system	L_e	R_{cs}	$L_e/2R_{cs}$ ($\cong P$)	n_p
CL-2-21	179	20.4	4.40	20.2
RS-8-21	122	19.1	3.17	42.2
CL-2-31	125	16.9	3.70	24.2

[a] All numerical values were evaluated so as to reproduce the measured values of R_g and R_h at 10 °C with eqs 9 and 10.

of the contour length L_e and the radius of cross section R_{cs} by[36]

$$R_{g,RR}^2 = \frac{\frac{4}{5}R_{cs}^5+(L_e-2R_{cs})R_{cs}^4+\frac{1}{3}(L_e-2R_{cs})^2R_{cs}^3+\frac{1}{12}(L_e-2R_{cs})^3R_{cs}^2}{(L_e-2R_{cs})R_{cs}^2+\frac{4}{3}R_{cs}^3} \quad (9)$$

The hydrodynamic radius, $R_{h,RR}$, for the rigid rod is expressed as follows according to the calculation by Norisue et al.:[37]

$$\frac{L_e}{2R_{h,RR}} = \ln\frac{2L_e-2R_{cs}+\{4L_e^2-4L_e(2R_{cs})+2(2R_{cs})^2\}^{1/2}}{2R_{cs}} + \frac{L_e+2^{1/2}(2R_{cs})-\{4L_e^2-4L_e(2R_{cs})+2(2R_{cs})^2\}^{1/2}}{L_e} + \frac{2R_{cs}}{2L_e}\ln\frac{(2^{1/2}-1)^2[2R_{cs}+\{4L_e^2-4L_e(2R_{cs})+2(2R_{cs})^2\}^{1/2}]}{2L_e-2R_{cs}+\{4L_e^2-4L(2R_{cs})+2(2R_{cs})^2\}^{1/2}} \quad (10)$$

Using eqs 9 and 10, we evaluated L_e and R_{cs} so as to reproduce the measured values of R_g and R_h at 10 °C. Results of the calculation are listed in Table 4, with the axis ratio $L_e/2R_{cs}$ and the number n_p of petals per flower. In all systems, the axis ratio, which corresponds to the flower number P, is larger than unity but not very large. The small number of flowers is consistent with the rigid rod structure assumed. The obtained R_{cs} values are in good agreement with the radii R_{star} of star-shaped polymers consisting of $2n_p + 2$ arms of molecular weight $M_{sc}/2$, which have been estimated from $R_{star}^2 = [(5/3)\text{-}R_{g,star}^2]^{0.5}$ to be 19.7, 17.9, and 16.3 nm for CL-2-21, RS-8-21, and CL-2-31, respectively. In evaluating the agreement of R_{cs} with R_{star}, however, we have to take into consideration the finite size of the core at the center of flower. The radius of the core was calculated to be 4.2 nm for CL-2-21, 5.2 nm for RS-8-21, and 4.5 nm for CL-2-31 on the assumption that the PS core was not swollen with solvent. The R_{cs} values expected from a simple addition of the core size to R_{star} exceed those obtained above by the model calculation. However, the presence of the core of finite size has to bring about relaxation of the stretching of the grafted chains and reduce the length of the petals in the flower. Therefore, the agreement of R_{cs} with R_{star} may imply the cancelation of these two effects of the core of finite size.

The above discussion can be summarized as follows. The magnitude of measured R_g cannot be explained by any model structures of a single flower, a collapsed network chain of flowers including microgel, and a flexible string of flowers, but can be explained by the rigid rod structure. Therefore, the most likely structure is the rigid rod-like string of a few flowers. On the basis of this structure, the estimated behavior of unimolecular micelle formation as a function of branch density and solvent quality is presented in the following.

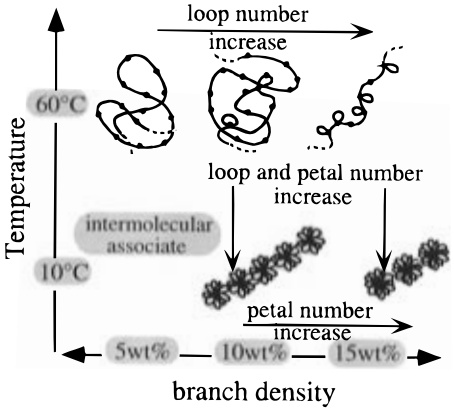

Figure 12. Schematic illustration of estimated structures of PMMA-*g*-PS at solvent composition [AN]:[AAEE] = 2:1 as a function of temperature and branch density. Intramolecular associations starts to take place at a branch density between 6 and 12 wt %. At higher branch densities and lower temperatures, unimolecular micelles of rigid rod structure made of a few linearly connected flowers are formed. Number of petals per flower increases with decrease of temperature and/or increase of branch density. At the lower branch density, with decreasing temperature, multimolecular associates are formed via random coil structure with shrunken branch chains.

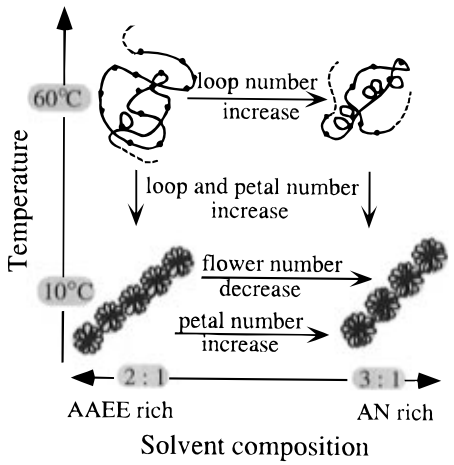

Figure 13. Schematic illustration of estimated structures of PMMA-*g*-PS CL-2 in AN/AAEE mixed solvents as a function of temperature and solvent composition. Numbers of loops per chain and petals per flower increase with decrease of temperature and/or increase of AN composition.

Formation of Unimolecular Micelles by Intramolecular Associations. In Figures 12 and 13 are illustrated predicted structures of graft copolymers as diagrams of temperature−branch density and temperature−solvent composition, respectively.

Introduction of associative branches to the backbone chain leads to the formation of loops (or petals) by intramolecular associations between grafted branches. At the solvent composition of [AN]:[AAEE] = 2:1, the loop formation starts to take place at a branch density between those of CL-1 and CL-2, i.e., between 6 and 12 wt %. In CL-2-21, the loops may already be formed at higher temperatures, which brings about chain shrinkage and topological repulsive interaction between segmental chains.[38−40] These two effects of loop formation result in the R_g similar to that of CL-b-21. With decreasing temperature, which implies the decrease of excluded volume of the backbone chain and the increase of attractive interaction between branch segments, the

loop number increases, and a flexible chain of flowers with a few petals may be formed. With a further decrease of temperature, n_p increases, P decreases, and the contour length and the flexibility of unimolecular micelle decrease. Eventually, the rigid rod structure consisting of about five flowers is formed around 10 °C.

The intramolecular association proceeds with an increase of branch density as well. For example, at 10 °C, the contour length L_e for RS-8-21 is shorter than that for CL-2-21 by 40%, and the number of petals for RS-8-21 is about 2 times larger than that for CL-2-21- (see Table 4).

The increase of AN composition brings about almost the same effects on micellar structure change as the decrease of temperature does, although the effects of solvent composition on the thermodynamical solvent quality for PMMA and PS are not equivalent to those of temperature, as mentioned before. Increase of AN composition results in shorter contour length and large petal number (compare the results for CL-2-31 and CL-2-21 in Table 4).

References and Notes

(1) Tuzar, Z.; Kratochivil, P. In *Surface and Colloid Science*; Matijevic, E., Ed.; Plenum Press: New York, 1993; Vol. 15, p 1.
(2) Leibler, L.; Oriand, H.; Wheeler, J. C. *J. Chem. Phys.* **1983**, *79*, 3550.
(3) ten Brinke, G.; Hadziioannou, G. *Macromolecules* **1987**, *20*, 1986.
(4) Honda, C.; Sakaki, K.; Nose, T. *Polymer* **1994**, *35*, 5309.
(5) Honda, C.; Hasegawa, Y.; Hirunuma, R.; Nose, T. *Macromolecules* **1994**, *27*, 7660.
(6) Balsara, N. P.; Tirrell, M.; Lodge, T. P. *Macromolecules* **1991**, *24*, 1975.
(7) Zhou, Z.; Chu, B.; Peiffer, D. G. *Macromolecules* **1993**, *26*, 1876.
(8) Raspand, E.; Lairez, D.; Carton, J.-P. *Macromolcules* **1994**, *27*, 2956.
(9) Selb, J.; Gallot, Y. In *Polymeric Amines and Ammonium Salts*; Goethals, E. J., Ed.; Pergamon Press: Oxford, 1980.
(10) Price, C.; Woods, D. *Polymer* **1973**, *14*, 82.
(11) Gallot, T.; Franta, E.; Remp, P.; Benoit, H. *J. Polym. Sci. Part C* **1964**, *4*, 473.
(12) Dondos, A.; Remp, P.; Benoit, H. *J. Chim. Phys.* **1965**, *62*, 821.
(13) Bresler, S. E.; Pyrkov, L. M.; Frenkel, S. Ya.; Laius, L. A.; Klenin, S. I. *Vysokomol. Soedin.* **1962**, *4*, 250.
(14) Halperin, A. *Macromolecules* **1991**, *24*, 1418.
(15) Kikuchi, A.; Nose. T. *Polymer*, in press.
(16) Semenov, A. N.; Joanny, J.-F.; Khokhlov, A. R. *Macromolecules* **1995**, *28*, 1066.
(17) de Gennes, P. G. *Isr. J. Chem.* **1995**, *35*, 33.
(18) Kikuchi, A.; Nose, T. *Polymer* **1995**, *36*, 2781.
(19) Varma, B.; Fujita, Y.; Takahashi, M.; Nose, T. *J. Polym. Sci., Polym. Phys. Ed.* **1984**, *22*, 1181.
(20) Benoit, H.; Froelich, D. In *Light Scattering from Polymer Solutions*; Huglin, M. B., Ed.; Academic Press: New York, 1972; Chapter 11.
(21) Brunel, R. F.; Bibber, K. V. In *International Critical Tables*; West, C. J., Dorsy, N. E., Chowsky, F. R. B., Klemenc, A. K., Eds.; McGraw-Hill: New York, 1926; Vol. 3, p 27.
(22) Dixon, A. L.; West, C. J. In *International Critical Tables*; West, C. J., Dorsy, N. E., Chowsky, F. R. B., Klemenc, A. K., Eds.; McGraw-Hill: New York, 1930; Vol. 7, p 34.
(23) Koppel, D. E. *J. Chem. Phys.* **1974**, *57*, 4814.
(24) Elias, H. G. In *Polymer Handbook*, 3rd ed.; Brandrup, J., Immergut, E. H., Eds.; Wiley: New York, 1989; Chapter 3.
(25) de Gennes, P.-G. *J. Phys. Lett.* **1985**, *46*, 639.
(26) Grosberg, Y.; Nechaev, S. K.; Shakhnovich, E. I. *J. Phys. Fr.* **1988**, *49*, 2095.
(27) Yu, J.;Wang, Z. L.; Chu, B. *Macromolecules* **1992**, *25*, 1618.
(28) Chu, B.; Ying, Q.; Grosberg A. Y. *Macromolecules* **1995**, *28*, 180.
(29) Zimm, B. H.; Stockmayer, W. H. *J. Chem. Phys.* **1949**, *17*, 1301.
(30) Miyake, A.; Freed, K. F. *Macromolecules* **1983**, *16*, 1228.
(31) Douglas, J. F.; Freed, K. F. *Macromolecules* **1984**, *17*, 2344.
(32) Douglas, J. F.; Roovers, J.; Freed, K. F. *Macromolecules* **1990**, *23*, 4168.
(33) Roovers, J. E. L.; Toporowski, P.; Martin, J. *Macromolecules* **1989**, *22*, 1987.
(34) Takano, A.; Okada, M.; Nose, T. *Polymer* **1992**, *33*, 783.
(35) Numasawa, N.; Nose, T. *Macromolecules* **1986**, *19*, 593.
(36) Let the position of a point in the rod be expressed by a cylindrical coordinate (x,r) with the origin being taken at the center of the rod, the x-axis taken as the center axis of the rod, and r the radius. Then, the radius of gyration is expressed as

$$R_g^2 = \left[2\int_0^{(L_e-2R_{cs})/2}\int_0^{R_{cs}}(r^2+x^2)2\pi r\,dr\,dx + 2\int_0^{R_{cs}}\int_0^{r}\left\{(r^2-x^2)+\left(x+\frac{L-2R_{cs}}{2}\right)^2\right\}2\pi r\,dx\,dr\right] \Big/ \left[2\int_0^{(L_e-2R_{cs})/2}\pi R_{cs}^2\,dr + \int_0^{R_{cs}}4\pi r^2\,dr\right] \quad (11)$$

which leads to eq 9.
(37) Norisue, T.; Motowoka, M.; Fujita, H. *Macromolecules* **1979**, *12*, 320.
(38) Iwata, K.; Kimura, T. *J. Chem. Phys.* **1981**, *74*, 2039.
(39) Iwata, K. *Macromolecules* **1985**, *18*, 115.
(40) Roovers, J.; Toporowski, P. M. *Macromolecules* **1983**, *16*, 843.

MA9604808